ANL-6494

Argonne National Laboratory

CRITICAL STUDIES OF A FAST REACTOR CORE CONTAINING DEPLETED URANIUM AND SODIUM AS DILUENTS

(ZPR-III Assembly 36)

by

J. M. Gasidlo, J. K. Long,

and R. L. McVean

ANL-6494
Reactor Technology
(TID-4500, 17th Ed.)
AEC Research and
Development Report

ARGONNE NATIONAL LABORATORY
9700 South Cass Avenue
Argonne, Illinois

CRITICAL STUDIES OF A FAST REACTOR CORE CONTAINING DEPLETED URANIUM AND SODIUM AS DILUENTS

(ZPR-III Assembly 36)

by

J. M. Gasidlo, J. K. Long, and R. L. McVean

Idaho Division

January 1962

Operated by The University of Chicago
under
Contract W-31-109-eng-38

TABLE OF CONTENTS

LIST OF FIGURES

LIST OF TABLES

CRITICAL STUDIES OF A FAST REACTOR CORE CONTAINING DEPLETED URANIUM AND SODIUM AS DILUENTS

(ZPR-III Assembly 36)

by

J. M. Gasidlo, J. K. Long, and R. L. McVean

ABSTRACT

Critical studies were performed with a metallic, fast reactor core designed to investigate the effects of replacing highly absorbing U^{238} diluent with high-scattering, low-absorbing sodium diluent. The fuel was 15.7 w/o enriched U^{235} and the core contained 18.2 v/o sodium and 12.68 v/o stainless steel. The experimental program was designed to measure the effect of the material replacement on spectral indices, which consisted of the standard fission ratios, foil irradiations, and a large number of central reactivity coefficients. Other measurements included the Rossi-α, radial fission traverses, and edge reactivity worths of a few samples.

I. INTRODUCTION

Assembly 36 was similar to Assembly 22, a previous ZPR-III core described by Long et al.[1] Assembly 22 contained a 7:1 ratio of depleted to enriched uranium in the core. Assembly 36 was constructed by replacing a portion of the depleted uranium in the unit module of Assembly 22 with canned sodium. This reduced the ratio of depleted to enriched uranium to 5:1. The purpose was to determine the effect on the critical size and spectral indices caused by replacing highly absorbing diluent with highly scattering diluent.

II. DESCRIPTION OF ASSEMBLY 36

A. The ZPR-III Facility

The ZPR-III is a critical assembly divided into two halves for ease of loading. In the separated or shutdown state the value of k_{eff} is small. The principal feature of each half is a matrix consisting of a 31 x 31 array of horizontal stainless steel tubes, each 2.177 in. sq and 33.5 in. deep.

A complete set of neutron and gamma detectors, which drive the reactor instrumentation, is located on the top of each matrix, and five fuel-bearing control-safety rods enter each matrix from the rear. Figure 1 is a photograph of the machine. A complete description of the ZPR-III facility has been given by Cerutti et al.(2)

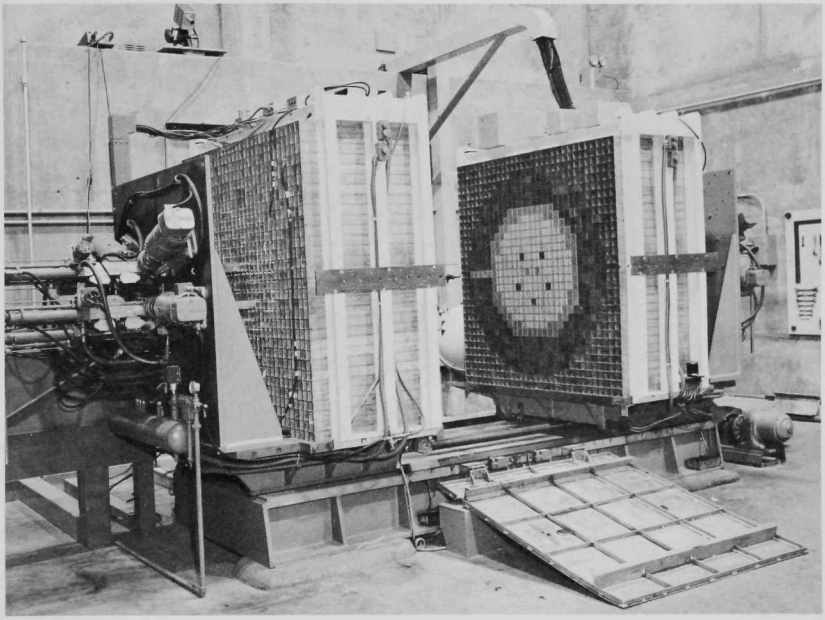

FIGURE 1

THE ZPR-III CRITICAL FACILITY

Reactor cores are simulated in the ZPR-III by loading drawers, containing core and blanket materials, into both matrices. Typical drawer loadings are shown in Fig. 2. Each core drawer is loaded with $\frac{1}{8}$-in.-thick plates of various materials, in the desired proportions and arrangement, to a length of half the core. Then the core drawers are inserted into the matrices in a repetitive pattern called the unit module. Each matrix contains half of the core, usually in the form of half of a horizontal cylinder, and the two halves are brought together to form the complete core assembly.

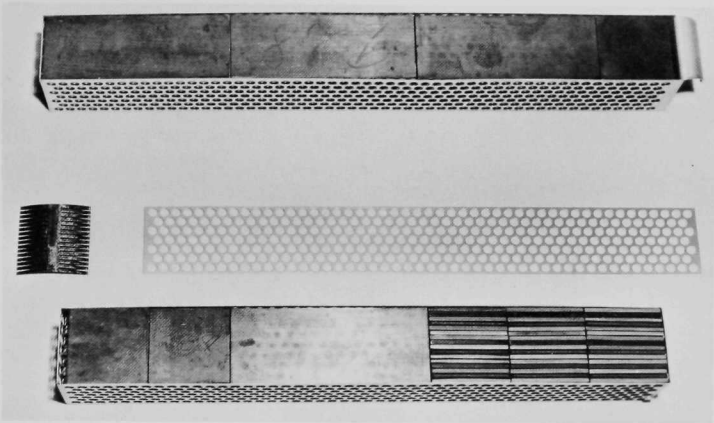

FIGURE 2

TYPICAL CORE AND BLANKET DRAWERS

B. The Unit Module of Assembly 36

The unit module of Assembly 36 was modeled from that of Assembly 22 to facilitate the comparison of results. The unit module of Assembly 22 consisted of a single drawer containing 2 columns of enriched uranium and 14 columns of depleted uranium loaded to a depth of 10 in., followed by the depleted uranium axial blanket. To form the unit module of Assembly 36, four columns of depleted uranium were removed and replaced with canned sodium. However, the inventory of sodium cans of the proper length was insufficient to load 10 in. of core in each drawer. Fourteen inches of core material per drawer was therefore chosen because of the availability of 7-in.-long sodium cans. Figure 3 is a top view of the core drawer loading master. The volume fractions of the unit module are given in Table I.

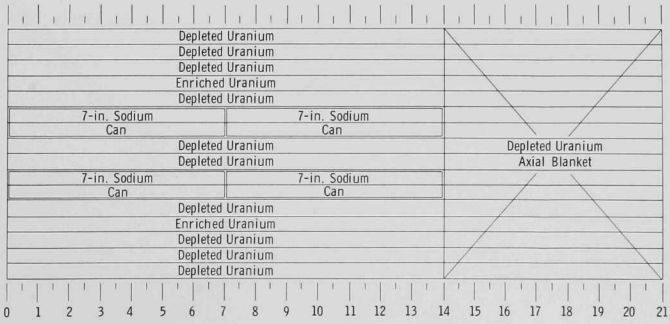

FIGURE 3

TOP VIEW OF THE CORE DRAWER LOADING MASTER

Table I

VOLUME FRACTIONS OF THE UNIT MODULE

Material	Assumed Density, gm/cm^3	Volume Fractions		
		Unit Module	DSN Calculation	Blanket
U^{235}	18.75	0.09374	0.0941	0.0019
U^{238}	19.0	0.5003	0.5050	0.8330
Na	0.84	0.1823	0.1840	-
Stainless Steel	7.85	0.1217	0.1218	0.0731

III. THE CRITICAL EXPERIMENT

A. Approach to Critical

The critical mass of Assembly 36 was calculated by the DSN code[3] using the 16-group cross-section set* of Yiftah, Okrent, and Moldauer.[4] The volume fractions used in the calculation of critical mass are also given in Table I. The calculated critical mass for a homogeneous sphere was 200.8 kg. Allowing a -5% correction in mass for heterogeneity and a +12% correction in mass for the conversion from a sphere to a cylinder, the estimated critical mass of Assembly 36 was therefore ~214 kg.

The approach to critical was performed in the usual manner of adding core drawers at the radial edge of the core. The graph of the approach to critical is shown in Fig. 4, and the outline of half No. 1 for the just-critical core is shown in Fig. 5.

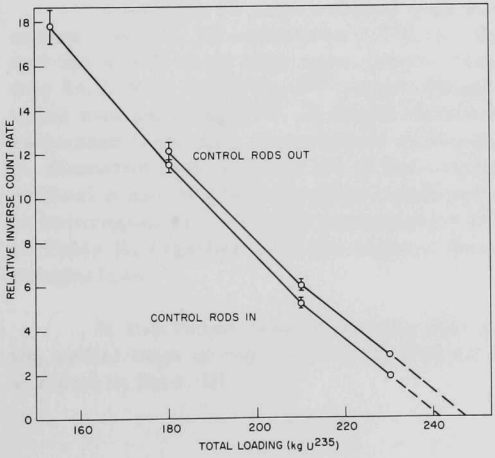

FIGURE 4

APPROACH TO CRITICAL

*Hereafter referred to as the YOM set.

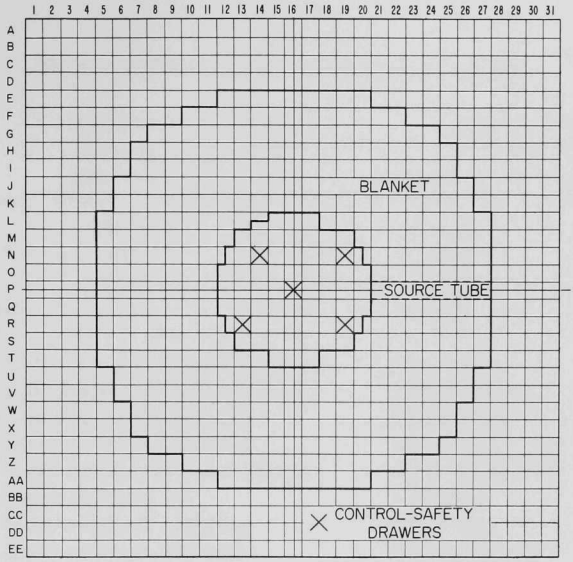

FIGURE 5

OUTLINE OF THE CRITICAL CORE HALF #1

B. Comparison of the Calculated and Experimental Values of the Critical Mass

Assembly 36 went critical with a total loading of 243.7 kg U^{235} and control rod No. 10 withdrawn 2.774 in. Using the control rod calibration and the worth of an edge core drawer (see Sect. III-C and D), the reactor was 44.7 Ih or 1.005 kg U^{235} supercritical. Therefore, the just-critical mass was 242.7 kg U^{235}. A shape-factor correction of 0.89 in mass was estimated from data reported by Loewenstein and Okrent[5] for the length-to-diameter ratio (L/D) 1.44 of the critical core. This yielded a calculated critical mass of 214.3 kg when combined with the -5% mass correction due to heterogeneity. Various parameters of the just-critical core are given in Table II, together with the volume fractions of Assembly 22 for comparison.

It was found experimentally that an increment of core material at the radial edge of the core was worth 42.4 Ih/kg on the average, as described in Sect. III-D.

Table II

PARAMETERS OF THE CRITICAL CORE

Material	Assumed Density, gm/cm^3	Total Mass, kg	Volume Fractions	
			Assembly 36	Assembly 22
U^{235}	18.75	243.70	0.09372	0.0942
U^{238}	19.0	1,304.65	0.4951	0.701
Na	0.84	21.234	0.1823	-
Stainless Steel	7.85	138.07	0.1268	0.093

Calculated Critical Loading	214.3 kg
Calculated Critical Volume	121.9 liters
Loading at Criticality	243.701 kg
Inhours Supercritical	44.7 Ih
Last Drawers Were Worth	44.5 Ih/kg U^{235}
Supercritical by	1.005 kg
Just-critical Loading	242.7 kg
Just-critical Volume	138.12 liters
Height	71.3 cm
Radius	24.8 cm
Radial Blanket	~35 cm
Axial Blanket	35.5 cm

If one inhour is taken to be worth $2.26 \times 10^{-5} \Delta k$, then the proportionality between edge core material and reactivity,

$$\frac{\Delta k}{k} = q \frac{\Delta M}{M} \quad ,$$

is established. Indeed, substituting the above figures in the relationship gives

$$42.4 \times 2.26 \times 10^{-5} = \frac{1}{242.7} q \quad ,$$

or a value of 0.234 for q. An approximate comparison can then be made between the observed critical configuration and the calculated multiplication of a blanketed sphere having the same composition and mass. The neutron multiplication of the sphere was calculated to be 1.031 by means of the YOM cross-section set, and the DSN code in the S8 approximation. With a shape-factor correction of 0.89, a heterogeneity correction of 1.05 (both figured on a mass basis), and the above value for q, the calculated k for the observed critical configuration was 1.016.

C. Control Rod Calibration

The control rod was calibrated in the usual manner by determining the period corresponding to an incremental change in the rod position. Core drawers were added at the radial edge to allow calibration over the central and outer portions of rod travel.

Effective delayed neutron fractions have been calculated for several of the ZPR-III assemblies. Using the data of Keepin et al.,[6] Meneghetti[7] has shown that the effective delayed neutron fractions of typical ZPR-III assemblies varies only slightly from a value of 0.0073. The calculated value for an assembly containing a 5:1 ratio of depleted to enriched uranium is 0.0074. Meneghetti[7] has also shown that the inhour curve is identical for a variety of ZPR-III assemblies in the period range of the rod calibration measurements (T>60 sec). Therefore, a ZPR-III inhour curve calculated for a prompt neutron lifetime of 8×10^{-8} sec and a total β_{eff} of 0.0073 was used to convert periods to inhours. The inhour curve is shown in Fig. 6 and the rod calibration in Fig. 7.

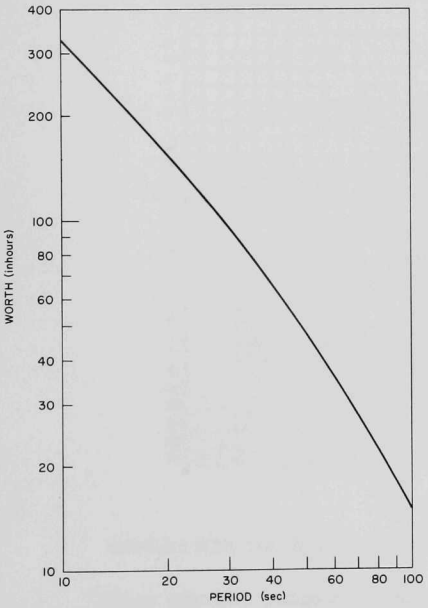

FIGURE 6
THE INHOUR CURVE

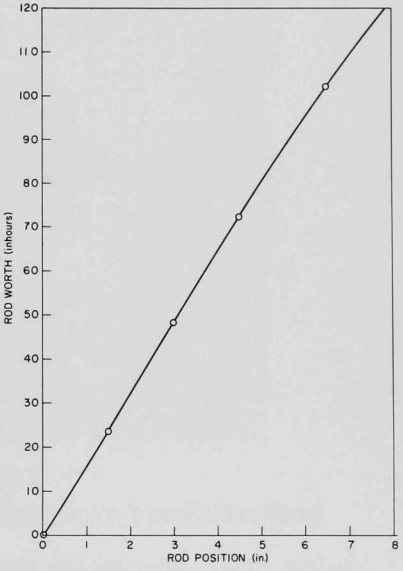

FIGURE 7
CONTROL ROD CALIBRATION

D. Worth of Edge Core Material

The outline of the critical core was "rounded-off," by means of the use of half-drawers. Since the sodium inventory is limited to 2-in.-high cans, horizontally divided half-drawers were formed by loading the plates of material across the drawer instead of in the usual vertical loading. With the fuel plates loaded horizontally in these drawers, an experiment was performed to determine whether or not there was a measurable effect from the different orientation. This was done by measuring the worths of a horizontally divided half-drawer and a vertically divided half-drawer in positions 1 and 2 of Fig. 8. These two locations reflect into each other on either side of a 45° line drawn through the center of the core, and hence any measurable difference between the worths of half-drawers loaded into these two positions should be entirely due to the difference in orientation of the fuel plates.

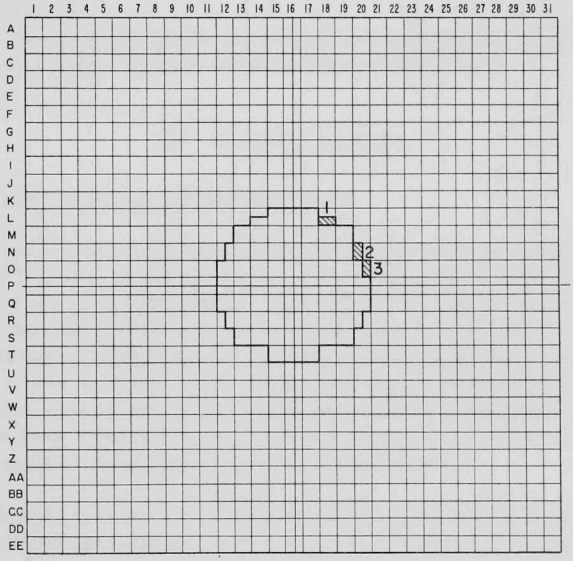

FIGURE 8

LOCATION OF EDGE CORE MATERIAL SUBSTITUTIONS

Since the fuel column is inside the sodium in the inner half of a vertically divided drawer and outside the sodium in the outer half of a vertically divided drawer, a third measurement was performed in position 3 to determine whether or not there was any significant effect due to material locations in the half-drawers.

The results of all the measurements are summarized in Table III.

Table III

EDGE CORE MATERIAL SUBSTITUTIONS (ASSEMBLY 36)

Drawer Location and Description	Worth* (Ih ± 0.5)	U^{235} Mass (kg)	Reactivity Coefficient (Ih/kg U^{235})	$q = \frac{\Delta k/k}{\Delta M/M}$
1. Inner half of a horizontally divided drawer	85.4	1.9194	44.5 ± .3	0.245 ± 0.002
2. Inner half of a vertically divided drawer	81.6	1.9194	42.5 ± .3	0.234 ± 0.002
3. Outer half of a vertically divided drawer	77.4	1.9194	40.3 ± .3	0.222 ± 0.002

*The ± 0.5 uncertainty in the reactivity measurement is described in Sect. VI in the discussion on reactivity coefficients.

IV. FISSION RATIOS

A. Central Fission Counter Measurements

The experimental fission ratios were determined from absolute fission counters[8] (2 in. in diameter by 1 in. long) loaded into the first inch of the central drawer in each half. The same U^{235} fission counter was maintained in one half while counters containing various fissionable materials were alternately loaded into the other half. The measurements were made at power levels of 0.5 to 10 watts, and the data were reported as the ratio of the total counts of a given counter to the standard U^{235} counter. The data were then reduced by a set of simultaneous linear equations involving the isotopic concentrations of the counters.

The central fission ratios were calculated from the central neutron spectra of the DSN calculations and the YOM cross-section set. The central neutron spectra of Assemblies 22 and 36 are given in Table IV for reference. The calculated and measured fission ratios are summarized in Table V.

Table IV

CALCULATED CENTRAL NEUTRON SPECTRA OF ASSEMBLIES 22 AND 36

Group	Lower Energy Limit (Mev)	Assembly 36	Assembly 22*	Group	Lower Energy Limit (Mev)	Assembly 36	Assembly 22*
1	3.668	0.0226	0.020	9	0.067	0.0498	0.048
2	2.225	0.0397	0.034	10	0.0407	0.0392	0.043
3	1.35	0.0625	0.054	11	0.025	0.0094	0.008
4	0.825	0.1146	0.109	12	0.015	0.0067	0.007
5	0.5	0.1927	0.199	13	0.0091	0.0018	0.002
6	0.3	0.2031	0.209	14	0.0055	0.0004	0
7	0.18	0.1527	0.157	15	0.0021	0	0
8	0.11	0.1052	0.108	16	0.0005	0	0

*Taken from Long et al.[1]

Table V

COMPARISON OF CENTRAL FISSION RATIOS
(Assemblies 22 and 36)

Isotope (i)	Assembly 36		Assembly 22[c]	
	Calculated[a]	Measured[b]	Calculated[a]	Measured
U^{233}	1.58	1.47 ± 1.4%	1.59	1.53
U^{234}	0.394	0.312 ± 1%	0.370	0.293
U^{236}	0.127	0.094 ± 1.1%	0.105	-
U^{238}	0.0469	0.041 ± 1.1%	0.040	0.036
Pu^{239}	1.25	1.19 ± 1.4%	1.24	1.16
Pu^{240}	0.387	0.337 ± 1%	0.366	0.333

[a] The YOM set was supplemented by values taken from BNL-325 cross sections for U^{234} and U^{236}.

[b] The limits quoted with the measured fission ratios represent 95% statistical confidence (two standard deviations) in the ratio of the total counts of the associated fission counters. These limits do not contain the uncertainties in the isotopic concentration of the fission counters.

[c] These values were taken from Long et al.[1] The data were taken so that the maximum uncertainty associated with the total counts of the fission counters is 1% for one standard deviation.

B. Foil Irradiations

Depleted and enriched uranium foils were irradiated in the core center and edge for radiochemical analysis to determine the U^{238}:U^{235} fission and capture ratios. Natural and enriched uranium foils were wrapped in aluminum foil and placed across the top of four core drawers at the midplane. Three enriched foils were placed across the top of core drawer 2-P-16 while three natural foils were placed on top of 1-P-16. Three enriched and natural foils were also placed across the top of core drawers 2-Q-16 and 1-Q-16 to provide average values for the core center. Similarly, a total of six enriched and six natural uranium foils were placed on top of core drawers 1-P-12, 2-P-12, 1-Q-12, and 2-Q-12 to provide average edge values (see Fig. 9). The foils were then irradiated for 20 watt-

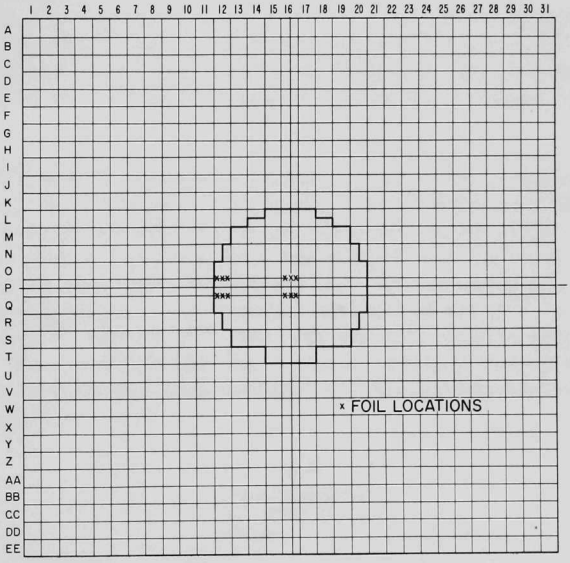

FIGURE 9

LOCATION OF FOILS DURING IRRADIATIONS

The radiochemical analysis of the foils was performed by S. B. Skladzien at Argonne, Illinois. The U^{238}:U^{235} fission and capture ratios were determined from the total induced activity of Mo^{99} and Np^{239}, respectively. The results are summarized and compared with calculations in Table VI.

Table VI

RESULTS OF FOIL IRRADIATIONS
(Assembly 36)

Location	Average Radius (cm)	$\frac{\sigma_f(U^{238})}{\sigma_f(U^{235})}$ Measured	$\frac{\sigma_f(U^{238})}{\sigma_f(U^{235})}$ Calculated*	$\frac{\sigma_c(U^{238})}{\sigma_f(U^{235})}$ Measured	$\frac{\sigma_c(U^{238})}{\sigma_f(U^{235})}$ Calculated*
Center	2.8	0.046 ± 7%	0.047	0.097 ± 5%	0.112
Edge	22.0	0.036 ± 7%	0.037	0.099 ± 5%	0.117

*These values were calculated from the central and edge neutron spectra of the "k" calculation and the YOM cross-section set.

V. RADIAL FISSION TRAVERSES

The blanket and core drawers in half No. 2, column 16 (see Fig. 5) were modified to accept a 1.27-cm-OD vertical thimble approximately 0.8 cm back of the midplane. Thus, as the fission counters were driven down through the thimble, they passed between large parallel sheets of core material formed by the vertically loaded plates in each drawer lining up throughout the core.

The U^{235} and U^{238} fission counters were 1.1 cm in diameter with active volumes of 5.1 cm in length. The traverse mechanism was set so that the center of the radial traverse occurred when the center of the active volume of the fission counter was located at the midplane of the core. Thus, the data represent fission rates integrated over 2.5 cm on either side of the indicated radial position. The isotopic analysis of the U^{235} counter was 93.2% U^{235}, 6% U^{234}, and 1% U^{238}, whereas the U^{238} counter contained only 80 ppm U^{235}. No correction for the minority isotopes has been applied to the data. The results are summarized in Table VII and shown graphically in Figs. 10 and 11.

Table VII

RADIAL FISSION TRAVERSES
(Assembly 36)

Fission Counter Position (cm)	U^{235} Traverse Total Counts	U^{235} Traverse Normalized	U^{238} Traverse Total Counts	U^{238} Traverse Normalized
58.4	(Void/Blanket Interface)			
55.8	904 ± 3.9%	0.027 ± 0.001	63 ± 12.6%	0
45.7	2,753 ± 2.6%	0.082 ± 0.002	310 ± 5.7%	0.010 ± 0.001
35.6	6,922 ± 2.2%	0.205 ± 0.005	1,398 ± 2.7%	0.044 ± 0.001
25.4	17,187 ± 2.0%	0.510 ± 0.010	9,842 ± 1.1%	0.310 ± 0.003
24.8	(Blanket/Core Interface)			
20.3	22,533 ± 1.9%	0.669 ± 0.013	18,364 ± 0.9%	0.579 ± 0.005
15.2	27,373 ± 1.9%	0.812 ± 0.015	24,281 ± 0.8%	0.766 ± 0.006
10.2	31,417 ± 1.9%	0.932 ± 0.018	28,464 ± 0.8%	0.898 ± 0.007
7.6	32,364 ± 1.9%	0.960 ± 0.018	29,873 ± 0.8%	0.942 ± 0.008
5.1	32,886 ± 1.9%	0.976 ± 0.018	30,719 ± 0.8%	0.969 ± 0.008
2.5	34,034 ± 1.9%	1.010 ± 0.019	31,366 ± 0.8%	0.989 ± 0.008
0	33,300 ± 1.9%	0.988 ± 0.018	31,982 ± 0.8%	1.008 ± 0.008
2.5	34,418 ± 1.9%	1.021 ± 0.019	31,204 ± 0.8%	0.984 ± 0.008
5.1	32,926 ± 1.9%	0.977 ± 0.018	30,675 ± 0.8%	0.967 ± 0.008
7.6	31,520 ± 1.9%	0.935 ± 0.018	29,343 ± 0.8%	0.925 ± 0.007
10.2	29,842 ± 1.9%	0.885 ± 0.017	28,669 ± 0.8%	0.904 ± 0.007
15.2	26,594 ± 1.9%	0.789 ± 0.015	23,341 ± 0.8%	0.739 ± 0.006

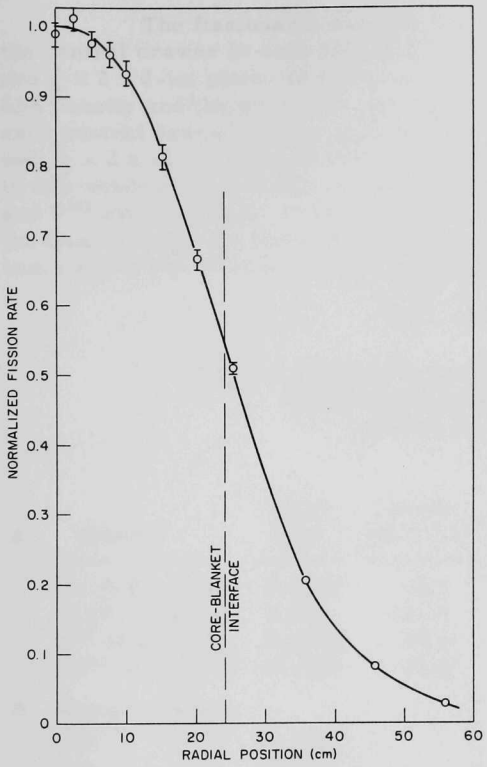

FIGURE 10

U^{235} RADIAL FISSION RATE TRAVERSE

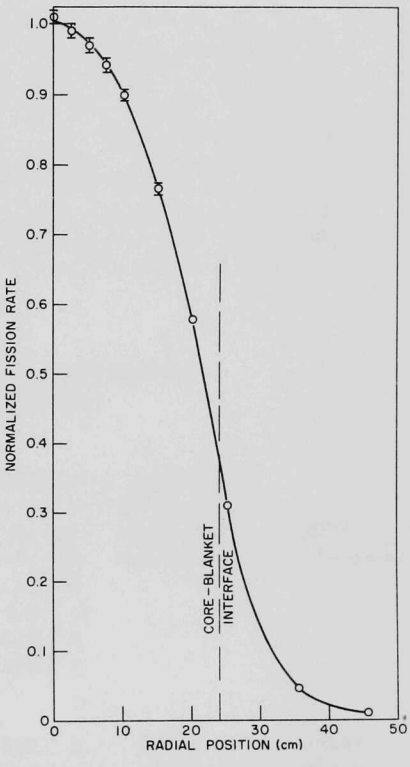

FIGURE 11

U^{238} RADIAL FISSION RATE TRAVERSE

VI. REACTIVITY COEFFICIENTS

A. Central Reactivity Worths

1. Measurements

The central reactivity measurements in ZPR-III normally fall into two groups, one of small volume (2 $in.^3$) fissionable samples and the other of larger volume (8 $in.^3$) nonfissile samples. The nonfissile materials require larger samples due to their generally low worths in fast cores.

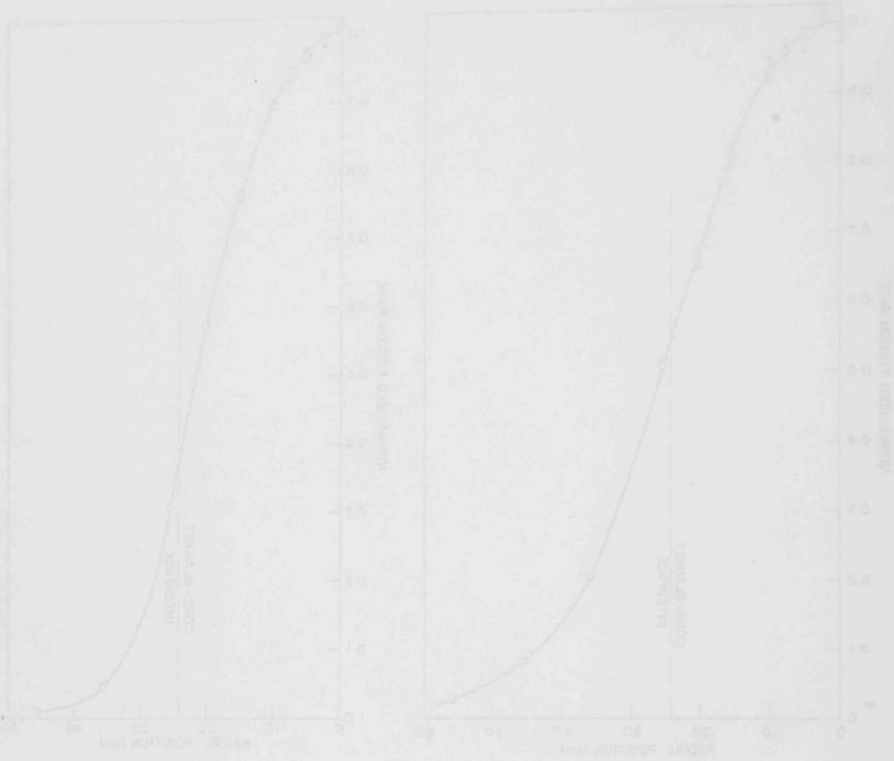

The fissionable samples were loaded across the front $\frac{1}{4}$ in. of the central drawer in each half of the core. The reference was run with two $\frac{1}{8}$ x 2 x 2-in. plates of aluminum loaded in each central drawer, one of 63% density and the other 45% density. The enriched uranium sample in each central drawer consisted of one $\frac{1}{8}$ x 2 x 2-in. plate sandwiched between two $\frac{1}{16}$ x 2 x 2-in. plates of 100%-density aluminum. The aluminum mass in this sandwich was nearly equal to that of the reference run. The Pu^{239} and U^{233} samples were contained in $\frac{1}{4}$ x 2 x 2-in. aluminum cans. Again, the total mass of the aluminum cans was nearly equal to that of the aluminum used in the reference. The measured values are given in Table VIII.

Table VIII

CENTRAL REACTIVITY COEFFICIENTS OF FISSIONABLE MATERIALS
(Assembly 36)

A. Sample	Mass (kg)	Worth (Ih ± 0.5)	Reactivity Coefficient (Ih/kg)	Reactivity Coefficient (Ih/g-mole)	R[c]
93.1% Enriched	0.2878	60.5	210 ± 2		
99.8% Depleted	2.378	-21.9	-9.2 ± .2		
U^{233} Mixture[a]	0.2266	94.6	418 ± 2		
Pu^{239} Mixture[b]	0.1860	71.5	384 ± 3		
B. Isotopic Values					
U^{235}	0.2684		225 ± 2	52.9 ± .5	0.03583
U^{238}	2.373		-9.7 ± .2	-2.78 ± .05	0.00368
U^{233}	0.2212		428 ± 2	99.8 ± .5	0.03381
Pu^{239}	0.1758		402 ± 3	96.1 ± .7	0.03390

(a) The isotopic concentrations were 97.40% U^{233} and 2.60% U^{238}. The isotopic value was calculated assuming that all of the reactivity effect was due to the U^{233}.

(b) The isotopic concentrations were 94.51% Pu^{239}, 5.11% Pu^{240}, and 0.38% Pu^{241}. The isotopic value was calculated assuming that Pu^{240} has approximately $\frac{1}{5}$ the worth of Pu^{239}.

(c) R is the ratio of $[(\nu-1)\,\sigma_f - \sigma_c]$ (calculated) to the observed worth in Ih/g-mole.

Special drawers were loaded into the central matrix tube in each half for the nonfissile sample measurements. These drawers allow 2 x 2 x 1-in.-thick samples to be inserted and removed in the first inch of the drawer without removing the core drawer. The reference was run with the sample volume void and all of the values reported are relative to void.

A sample of depleted uranium of large volume was included in this series of measurements because of the large uncertainty in the worth of a small sample. The boron carbide samples contained 9.9% chemical impurities which were regarded as making no measurable contribution to the reactivity worth. The boron was enriched to 90.7 a/o in B^{10}, but the results are based on the total amount of boron carbide in the sample, with an assigned molecular weight of 52. The physicum samples, designated Ph-I and Ph-II, are mixtures of metals, oxides, and salts of stable, naturally occurring elements selected to simulate the nuclear effects of fission products according to criteria listed in a paper by Long et al.(9) The formulae of these two mixtures corresponded to (Ph-I) $O_{1.519}$ and (Ph-II) $O_{1.146}$ with molecular weights of 142.2 and 136.1, respectively. The results of the nonfissile sample measurements are given in Table IX.

Table IX

CENTRAL REACTIVITY COEFFICIENTS OF NONFISSILE MATERIALS

Sample	Mass (kg)	Worth (Ih ± 0.5)	Reactivity Coefficient (Ih/kg)	Reactivity Coefficient (Ih/g-mole)	$-\sigma_{eff}$ (mb/atom)
Al	0.3506	- 4.6	-13.1 ± 1.4	-0.35 ± 0.04	-12 ± 1.3
SS	1.0172	-12.5	-12.3 ± 0.5	-0.69 ± 0.03	-23.4 ± 0.9
C	0.1964	~0.1	~0.5 ± 2.5	0.006 ± 0.03	0.2 ± 1.0
Na(a)	0.0912	- 0.4	-4.4 ± 5.5	-0.10 ± 0.13	-3.4 ± 4.4
Al_2O_3	0.3551	- 2.8	-7.9 ± 1.4	-0.81 ± 0.14	-27 ± 5
Be	0.2407	8.9	37 ± 2	0.33 ± 0.02	11.3 ± 0.6
Li(a)	0.0549	-11.9	-217 ± 9	-1.51 ± 0.06	-51 ± 2
Nb(a)	0.4896	-15	-30.6 ± 1	-2.84 ± 0.09	-96 ± 3
Ph-I(a)*	0.232	- 6.7	-28.9 ± 2.2	-4.1 ± 0.3	-140 ± 11
Ph-II(a)*	0.210	- 6.7	-31.9 ± 2.4	-4.3 ± 0.3	-148 ± 11
Mo	1.2798	-26.6	-20.8 ± 0.4	-2.00 ± 0.04	-68 ± 1.3
Y	0.5821	- 4.2	-7.2 ± 0.9	-0.64 ± 0.08	-22 ± 3
Ag	0.6831	-46.8	-68.5 ± 0.7	-7.39 ± 0.08	-251 ± 3
Ta(a)	1.0044	-41.2	-41 ± 0.5	-7.42 ± 0.09	-252 ± 3
$B^{10}C$*	0.03217	-55.9	-1,928 ± 17	-100.3 ± 0.9	-3400 ± 31
Th^{232}	1.5117	-32.6	-21.6 ± 0.3	-5.01 ± 0.07	-170 ± 2.4
CH_2	0.00687	6.8	990 ± 73	14 ± 1	475 ± 34
Pb	1.475	- 3.2	-2.2 ± 0.3	-0.46 ± 0.06	-15 ± 2
Zr	0.8460	- 6.7	-7.9 ± 0.6	-0.72 ± 0.06	-24 ± 2
Bi	1.2762	- 2.8	-2.2 ± 0.4	-0.46 ± 0.08	-16 ± 3
O			-2.1 ± 3.4	-0.034 ± 0.054	1.1 ± 1.8

(a) These samples were canned in stainless steel. The sample mass is that of the named material only. The sample worth has been corrected for the effect of the stainless steel, and the reactivity coefficient is for the named material only.

*These samples are described in the text.

The reactivity worths were determined from the difference in the critical position of the control rod for the sample and reference runs. In ZPR-III, the control rods (fuel-removal type) must be withdrawn and the halves of the reactor must be separated to insert the sample. Reproducibility in the control rod position is better than ± 0.005 in. (less than ± 0.1 Ih), whereas the uncertainty in the closure of the halves is ± 0.5 Ih. The uncertainties in the reactivity coefficients were calculated from the latter value.

2. Comparison of Results

The sample worths and reactivity coefficients of Assemblies 22 and 36 can be compared directly because of the nearly identical critical masses and volumes. However, a simple comparison can be made between reactors of differing sizes through the use of one-energy-group perturbation theory. In the first-order approximation, the reactivity effect of a fissile sample can be described by the equation

$$\frac{\Delta k}{k} = \frac{\int_{\text{sample}} [(\nu-1)\sigma_f - \sigma_c]\, \phi^2(r)\, N_s\, dV}{\int_{\text{core}} \nu\sigma_f\, \phi^2(r)\, N_c\, dV} \quad ,$$

The denominator is a constant for a specific core and, if the sample volume is in the center of the core where the spatial flux distribution can be normalized to 1, the equation can be written as:

$$\frac{\Delta k}{k} = \frac{1}{A} \overline{[(\nu-1)\, \sigma_f - \sigma_c]}\, N_t \quad ,$$

where

$$A = \int_{\text{core}} \nu\sigma_f\, \phi^2(r)\, N_c\, dV \quad ,$$

$$\overline{[(\nu-1)\, \sigma_f - \sigma_c]} = \sum_{j=i}^{n} [(\nu_j - 1)\, \sigma_{f_j} - \sigma_{c_j}]\, \phi_j \quad ,$$

N_t = number of atoms in the perturbation sample .

For nonfissile samples, for which ν and σ_f are 0, the equation reduces to

$$\frac{\Delta k}{k} = \frac{1}{A} (-\sigma_{\text{eff}})\, N_t \quad ,$$

where σ_{eff} is an effective cross section, which includes the effects of energy downscattering. The central reactivity worth can be expressed in this form, since there is no contribution from the transport cross section due to the zero flux gradient.

The average value $\overline{[(\nu-1)\ \sigma_f - \sigma_c]}$ was calculated from the central DSN spectrum (see Table IV) for each of the fissile samples. These results are tabulated in column R of Table VIII. The effective cross sections were calculated by multiplying each reactivity coefficient by $[(\nu-1)\ \sigma_f - \sigma_c]$/lh/g-mole ($Pu^{239}$) because the relatively high and constant cross section of Pu^{239} in the high-energy range is less susceptible to errors in the neutron energy spectrum. A value of $-\sigma_{eff}$ was calculated for each of the reactivity samples measured in Assembly 36. These values are included in Table IX. A comparison of the effective cross sections of reactivity samples measured in both Assemblies 22 and 36 are given in Table X.

Table X

COMPARISON OF EFFECTIVE CROSS SECTIONS IN ASSEMBLIES 22 AND 36

Material	$-\sigma_{eff}$ (mb/atom) 22	36
U^{233}	3284 ± 15	3383 ± 17
U^{235}	1772 ± 12	1793 ± 17
U^{238}	-84 ± 2	-94.2 ± 1.7
Pu^{239}	3238 ± 17	3258 ± 24
C	-10.8 ± 0.9	0.2 ± 1
Al	-13.1 ± 1.2	-12 ± 1.3
SS	-23.8 ± 0.9	-23.4 ± 0.9
Zr	-34.7 ± 1.5	-24 ± 2
Ag	-231 ± 1.2	-251 ± 3
Bi	-27 ± 3	-16 ± 3
Y	-30 ± 3	-22 ± 3
Be	-4.8 ± 0.6	11.3 ± 0.6
$B_4^{10}C$	-3130 ± 26	-3400 ± 31

B. Edge Measurements

The worths of a number of reactivity samples were measured near the edge of the core in core drawers 1 and 2-P-13 (see Fig. 12). Both the fissile and nonfissile measurements were performed exactly as described for the central measurements, and all comments on the central worths are equally applicable to the edge values. The results of the edge measurements are summarized in Table XI.

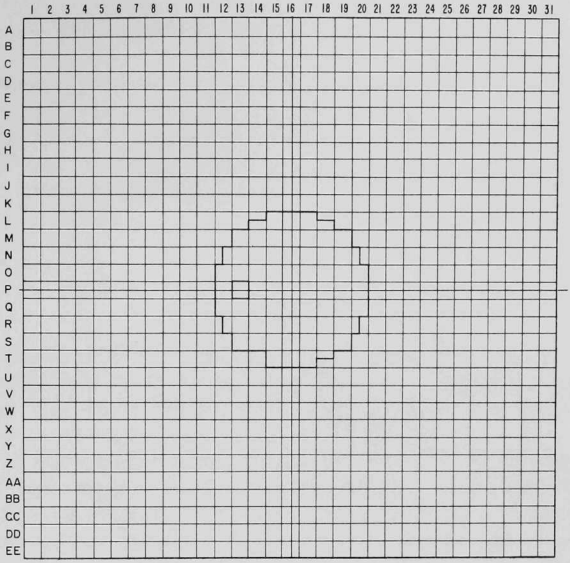

FIGURE 12

LOCATION OF REACTIVITY MEASUREMENTS

Table XI

EDGE REACTIVITY COEFFICIENTS

Sample	Mass (kg)	Worth (Ih ± 0.5)	Reactivity Coefficient (Ih/kg)	Reactivity Coefficient Ih/g-mole
93.1% Enriched	0.2878	35.9	125 ± 2	
99.8% Depleted	2.3780	-1.5	-0.63 ± 0.21	
U^{233} Mixture	0.2266	54.1	239 ± 2	
Pu^{239} Mixture	0.1860	42.3	227 ± 3	
Isotopic Values				
U^{235}	0.2684		134 ± 2	31.5 ± 0.5
U^{238}	2.3730		-0.91 ± 0.21	-0.22 ± 0.05
U^{233}	0.2212		246 ± 2	57.3 ± 0.5
Pu^{239}	0.1758		238 ± 3	56.9 ± 0.7
Nonfissile Materials				
Al	0.3506	5.0	14.3 ± 1.4	0.39 ± 0.04
SS	1.0172	2.7	2.7 ± 0.5	0.15 ± 0.03
Na	0.0912	1.8	20 ± 6	0.46 ± 0.14
Al_2O_3	0.3551	7.2	20.3 ± 1.4	2.07 ± 0.14
Th^{232}	1.4885	-10.2	-6.9 ± 0.3	-1.60 ± 0.07
O			28.6 ± 3.4	0.46 ± 0.05

VII. PROMPT NEUTRON LIFETIME

The average prompt neutron lifetime was determined by the Rossi-α method. The equipment and the experimental technique have been described by Brunson et al.[10] The measured Rossi-α at delayed critical was $(9.4 \pm 0.1) \times 10^4$ sec^{-1}. For an effective β of 0.0074 ± 4%, calculated for a 5:1 ratio of enriched to depleted uranium, the prompt neutron lifetime is $(7.9 \pm 0.4) \times 10^{-8}$ sec.

VIII. DISCUSSION

The primary effect of replacing part of the depleted uranium in Assembly 22 with sodium is an increase in the neutron flux in the high-energy region. The top three groups in the calculated spectra were 12 to 15% greater for Assembly 36 as compared with Assembly 22. Also, the fission ratios of the threshold detectors Pu^{240}, U^{234}, and U^{238} were greater by 1%, 3%, and 13%, respectively, in Assembly 36. The measured U^{233} fission ratio decreased slightly, whereas that of Pu^{239} was increased slightly. This is probably due to the shift in neutrons up to the high-energy groups, maintaining the Pu^{239} fission rate due to its constant cross section in that region, while decreasing the U^{235} fission rate due to its decreasing cross section.

It is also interesting to note that the effective cross sections in Assembly 36 were generally similar to those in Assembly 22, with two outstanding exceptions for carbon and beryllium. The amount of depleted uranium removed must have been sufficient to result in a balance between the increased absorption in the U^{238} and the increased fission rate in the U^{235} because of the general degradation of the neutron spectrum by the carbon. The larger increase in the worth of the beryllium sample is probably due to a similar condition accompanied with an increased (n,2n) reaction rate because of the increased proportion of neutrons in the high-energy groups.

ACKNOWLEDGMENTS

The authors wish to thank F. W. Thalgott for his guidance in the experimental program which includes this assembly, W. P. Rosenthal for his aid in editing this report, and the technicians of the ZPR-III facility who contributed to the experiments.

REFERENCES

1. J. K. Long, A. R. Baker, W. Gemmell, W. P. Keeney, R. L. McVean, and F. W. Thalgott, Experimental Results on Large Dilute Fast Critical Systems with Metallic and Ceramic Fuels, P/SM-18/48, Seminar on the Physics of Fast and Intermediate Reactors, Vienna (August, 1961).

2. B. C. Cerutti et al., ZPR-III, Argonne's Fast Critical Facility, Nuc. Sci. and Eng., 1, 126 (1956).

3. B. G. Carlson et al., The DSN and TDC Neutron Transport Codes, LAMS-2346 (1960).

4. S. Yiftah, D. Okrent, and P. A. Moldauer, Fast Reactor Cross Sections, A Study Leading to a 16-group Set, Pergamon Press, New York (1960).

5. W. B. Loewenstein and D. Okrent, The Physics of Fast Power Reactors; A Status Report, Proceedings of the Second United Nations International Conference on the Peaceful Uses of Atomic Energy, Geneva, Switzerland, 12, 22 (1958).

6. G. R. Keepin, T. F. Wimett, and R. K. Zeigler, Delayed Neutrons from Fissionable Isotopes of Uranium, Plutonium and Thorium, LA-2118 (1957).

7. D. Meneghetti, Recent Advances and Problems in Theoretical Analyses of ZPR-III Fast Critical Assemblies, P/SM-18/37, Seminar on the Physics of Fast and Intermediate Reactors, Vienna (August, 1961).

8. F. S. Kirn, An Absolute Fission Counter, Abstracts American Nuclear Society, 2nd Winter Meeting (October 28, 1957).

9. J. K. Long et al., Fast Neutron Power Reactor Studies with the ZPR-III, Proceedings of the Second United Nations International Conference on the Peaceful Uses of Atomic Energy, Geneva, Switzerland, 12, 119 (1958).

10. G. S. Brunson et al., Measuring the Prompt Period of a Reactor, Nucleonics, 15 (11), 132 (1957).